Available online at www.easd.procedia.org
EASD Procedia EURODYN (2026) 405-414

EASD Procedia

EURODYN 2026
XIII International Conference on Structural Dynamics
M. Beer, C. Papadimitriou, H. Jensen, J. Chen, M. Broggi, J. Behrensdorf (eds.)
Hannover, Germany, 27.09.–01.10 2026

INERTIAL AMPLIFICATION METASTRUCTURE ABSORBER FOR LIGHTWEIGHT VIBRATION CONTROL

Lanhe XU[1,2], Julien BROCAIL[2], Amine.MEHEL[3], Kuotian LI[2] and Bing LI[1]

[1] School of Aeronautics, Northwestern Polytechnical University,
Xi'an, Shaanxi 710072, China
e-mail: {lanhexu, bingli}@mail.nwpu.edu.cn

[2] ESTACA, ESTACA'Lab – laval
Rue Georges Charpak, F-53000, Laval, France
e-mail: {lanhe.xu, Julien.BROCAIL, kuotian.li}@estaca.fr

[3] ESTACA, ESTACA'Lab – Paris-Saclay
Montigny-le-Bretonneux, F-78180, France
e-mail: Amine.MEHEL@estaca.fr

Keywords: Inertial amplification, Metastructure, Vibration absorber, Low-frequency resonance, Particle swarm optimization, Lightweight vibration control.

Abstract. *Low-frequency flexural resonances in complex engineering piping systems pose severe threats to structural integrity. Traditional passive vibration control methods often require substantial parasitic mass, violating the stringent lightweight constraints in modern aerospace and transit applications. To overcome this fundamental bottleneck, this work proposes a novel inertial amplification metastructure absorber. By leveraging a meticulously designed kinematic topology, the mechanism geometrically amplifies a minimal physical mass into a massive apparent inertia under ungrounded boundary conditions. To achieve absolute suppression of the global maximum amplitude, an H_∞ norm optimization driven by the particle swarm optimization algorithm is conducted. The evolutionary process reveals the underlying physics of the inertial mechanism, demonstrating that minimizing the non-amplifiable top dead mass is imperative for maximizing the kinetic energy absorption capacity. The analytical model is thoroughly validated through three-dimensional finite element analysis. For a representative flexible pipe system, the proposed absorber operates under an extreme lightweight constraint with a mass ratio of approximately 0.5%, yet it successfully generates an apparent inertia that is more than four times its own physical mass. Acting as a highly efficient localized energy sink, the mechanism achieves a 46.5% reduction in the global maximum steady-state amplitude and exhibits rapid transient energy dissipation. This study provides a new paradigm for extreme lightweight vibration mitigation in complex engineering structures.*

ISSN:2311-9020 © 2026 The Authors. Published by EASD Procedia.
Peer-review under responsibility of the Organizing Committee of EURODYN 2026.
doi: 10.47964/1326.10669.219

1 INTRODUCTION

Modern engineering structures across a wide range of fields, such as aerospace, shipbuilding, and energy-chemical industries, are highly susceptible to low-frequency resonances induced by complex external excitation environments [1, 2]. Such low-frequency, large-amplitude dynamic responses not only accelerate structural fatigue evolution but can also directly trigger catastrophic system failures. When suppressing these low-frequency resonances, traditional tuned mass dampers (TMDs) are constrained by the physical laws of classical dynamic natural frequencies, necessitating the introduction of substantial parasitic mass [3, 4]. This conservative design, which incurs a severe mass penalty for vibration mitigation performance, severely deteriorates the static load-bearing environment of the primary structure and fundamentally contradicts the core development demands for extreme structural lightweighting in high-end equipment manufacturing.

In recent years, phononic crystals [5] and elastic metamaterials [6] have provided a revolutionary theoretical framework for low-frequency vibration mitigation and wave bandgap design, owing to their extraordinary wave-dynamic manipulation properties. Particularly, metastructures based on local resonance mechanisms can achieve effective attenuation of low-frequency elastic waves at sub-wavelength scales [7]. To further overcome the reliance of low-frequency locally resonant structures on large physical masses, inertial amplification (IA) metamaterials [8, 9] have gradually become a focal point at the forefront of mechanics. Through the kinematic coupling mechanisms of internal macroscopic or microscopic geometric configurations, IA metastructures can provide a virtual apparent mass hundreds of times greater than their actual physical weight. However, the physical installation of most existing classic IA structures, which are typically based on rack-and-pinion or ball-screw mechanisms, relies heavily on an absolutely stationary, external grounded reference point. For continuum structures with massive spatial spans and complex boundary conditions—such as beams, cables, and industrial piping—finding a reliable grounded anchor point in extreme deformation regions (e.g., mid-spans) often lacks feasibility in practical engineering layouts [10, 11]. Consequently, developing a structural IA vibration mitigation system that is entirely attached to the primary structure without the need for external grounding has emerged as a critical scientific challenge in the current field of lightweight vibration control for metamaterials.

Addressing the dual constraints of spatial layout and physical mass [12, 13], this paper proposes an ungrounded rhombus inertial amplification metastructure absorber, aiming to achieve highly efficient low-frequency resonance suppression in continuum structures under stringent mass limits. This metastructure system utilizes a purely geometric rigid linkage network to transform the minuscule longitudinal vibrations of the primary structure into drastic transverse motions of the laterally cross-coupled masses. This mechanism realizes an order-of-magnitude surge in the system's apparent inertia without relying on any external reference coordinate system. This deep coupling of asymmetric internal mass distribution and spatial geometric amplification thoroughly decouples the tuning frequency of the vibration mitigation system from the true physical dead weight, providing a novel mechanical architecture for achieving extreme low-frequency vibration suppression under ungrounded conditions.

This work aims to reveal the underlying kinematic principles of this ungrounded inertial metastructure and explore its performance limits under extreme lightweight objectives. First, a rigorous analytical model of the rhombus absorber unit is established based on Lagrange's dynamic equations to elucidate its intrinsic anti-resonance tuning mechanism. Subsequently, taking the low-frequency vibration of a typical industrial piping system as a representative engineering case, a swarm intelligence heuristic algorithm is introduced to perform a global parameter optimization for the metastructure under a strict total physical weight constraint. Finally,

three-dimensional continuum finite element harmonic sweep analysis is conducted to precisely validate the accuracy of the purely theoretical analytical model, as well as the outstanding efficacy of this lightweight metastructure in achieving absolute global peak suppression in real engineering continua.

2 KINEMATIC DESIGN AND DYNAMIC MODELING

2.1 Conceptual Design of the Ungrounded IAM Absorber

Aiming to address the low-frequency vibration mitigation of continuum structures under ungrounded conditions, this paper proposes a rhombus inertial amplification metastructure (IAM) absorber that is entirely attached to the primary structure without the need for external fixed reference points. The coupled system can be abstracted as a two-degree-of-freedom (2-DOF) dynamic model. It is assumed that the primary structure possesses an equivalent modal mass M and an equivalent modal stiffness K corresponding to its fundamental flexural vibration mode. The proposed ungrounded inertial mechanism is directly mounted at the location of maximum antinode amplitude of the primary structure via a single attachment point. The 3D conceptual schematic and the corresponding dynamic model of the proposed ungrounded inertial metastructure are illustrated in Figure 1(a).

This mechanism comprises four massless rigid links articulated to form a rhombus kinematic network. A linear tuning spring, with a stiffness denoted as k_a, is configured in parallel along the internal longitudinal diagonal of the rhombus linkage. To activate the inertial amplification effect, an asymmetric mass distribution strategy is implemented at the critical nodes of the rhombus mechanism. Specifically, a lumped mass, denoted as m_t, is positioned at the top vertex node of the mechanism. Meanwhile, two cross-coupled lateral masses, each denoted as m_s, are symmetrically distributed at the left and right horizontal expansion nodes of the rhombus linkage.

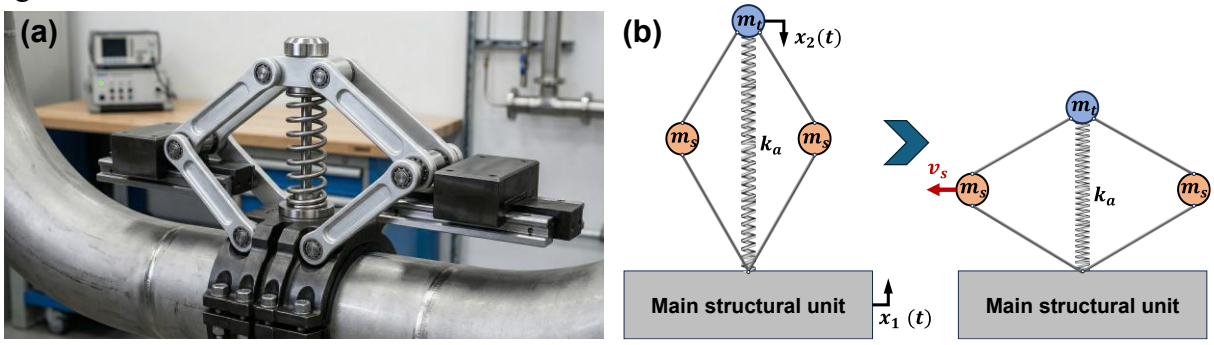


Figure 1: Design and Modeling. (a) 3D conceptual schematic of the ungrounded inertial metastructure. (b) Corresponding dynamic model and kinematic relationships.

2.2 Kinematic Analysis and Lagrangian Formulation

To establish the dynamic equations of the two-degree-of-freedom (2-DOF) system, the absolute longitudinal displacement of the primary structure and that of the absorber's top mass are defined as x_1 and x_2, respectively. The geometric configuration of the rhombus linkage mechanism dictates its internal kinematic amplification relationship. Based on the assumption of small-amplitude vibrations, the relative longitudinal deformation between the primary structure and the top mass is expressed as x_2-x_1. Constrained by the rigid links, the absolute motion velocity of the lateral nodes is synthesized from two mutually orthogonal components. The longitudinal translational velocity component equals the arithmetic mean of the velocities of the upper and lower nodes, given by $0.5(\dot{x_1}+\dot{x_2})$. The transverse ejection velocity component

is proportional to the relative longitudinal deformation velocity, with the proportionality constant being the amplification factor, denoted as α. Under the specific geometric design of this structure, the kinematic amplification factor remains constant at $\alpha = 2$. Consequently, the square of the absolute velocity of the lateral mass m_s can be formulated as the sum of the squares of its longitudinal and transverse velocity components.

$$v_s^2 = 4(\dot{x}_2 - \dot{x}_1)^2 + 0.25(\dot{x}_1 + \dot{x}_2)^2 \tag{1}$$

Based on the aforementioned kinematic analysis, the total kinetic energy T of the entire system is collectively composed of the primary structure, the top mass, and the two lateral masses, which can be expressed as:

$$T = \frac{1}{2}M\dot{x}_1^2 + \frac{1}{2}m_t\dot{x}_2^2 + m_s v_s^2 \tag{2}$$

By substituting the velocity expressions of the lateral masses and collecting like terms, the total kinetic energy T can be recast into a standard quadratic matrix form.

$$T = \frac{1}{2}(M + 8.5m_s)\dot{x}_1^2 + \frac{1}{2}(m_t + 8.5m_s)\dot{x}_2^2 - 7.5m_s\dot{x}_1\dot{x}_2 \tag{3}$$

The total potential energy U of the system is formulated by the elastic strain energy of both the primary structure's equivalent spring and the tuning spring.

$$U = \frac{1}{2}Kx_1^2 + \frac{1}{2}k_a(x_2 - x_1)^2 \tag{4}$$

By substituting the total kinetic and potential energies into Lagrange's equations for a conservative system, the matrix equations of motion for undamped free vibration can be derived.

$$[M]\begin{bmatrix}\ddot{x}_1\\ \ddot{x}_2\end{bmatrix} + [K]\begin{bmatrix}x_1\\ x_2\end{bmatrix} = \begin{bmatrix}0\\ 0\end{bmatrix} \tag{5}$$

The global mass matrix $[M]$ and the stiffness matrix $[K]$ of the system are respectively expanded into the following algebraic forms:

$$[M] = \begin{bmatrix}M + 8.5m_s & -7.5m_s\\ -7.5m_s & m_t + 8.5m_s\end{bmatrix} \tag{6}$$
$$[K] = \begin{bmatrix}K + k_a & -k_a\\ -k_a & k_a\end{bmatrix}$$

The diagonal elements of the mass matrix reveal that the lateral physical masses m_s induce a substantial apparent inertial amplification effect. Furthermore, the off-diagonal cross-coupling terms $-7.5m_s$ constitute the fundamental physical mechanism governing internal energy transfer and the ultimate suppression of the global resonance peak.

2.3 Eigenvalue Analysis and Anti-resonance Tuning Mechanism

The resonant frequencies and anti-resonance characteristics of the system can be obtained by solving the eigenvalue problem of the aforementioned dynamic matrices. By subjecting the primary structure to a harmonic excitation at frequency f and setting its longitudinal displacement x_1 to zero, the local anti-resonance frequency of the absorber subsystem can be analytically derived. At this specific frequency, the localized inertial force generated by the absorber perfectly counteracts the external excitation, thereby achieving highly efficient vibration mitigation for the primary structure. The analytical expression for the anti-resonance frequency

f_{valley} is fundamentally governed by the tuning spring stiffness and the equivalent apparent inertial mass of the absorber.

$$f_{valley} = \frac{1}{2\pi}\sqrt{\frac{k_a}{m_t + 8.5m_s}} \tag{7}$$

By solving the undamped eigenvalue equation of the system $|\boldsymbol{K} - \omega^2\boldsymbol{M}| = 0$, the two natural resonant frequencies can be further obtained, which correspond to the lower-bound frequency on the left and the upper-bound frequency on the right of the vibration suppression band. The spectral span between these two resonant frequencies defines the effective vibration suppression bandgap of the absorber. The analytical results reveal that the bandgap width is intimately correlated with the internal asymmetric mass distribution mechanism. This insight provides a robust theoretical underpinning for the subsequent global optimization of lightweight extremes under stringent mass constraints.

3 H_∞ DYNAMIC PARAMETER OPTIMIZATION VIA PARTICLE SWARM ALGORITHM

Following the construction of the kinematic relationships and the dynamic impedance matrix for the ungrounded inertial metastructure, the vibration suppression performance is strictly governed by the internal mass distribution and stiffness tuning. To meet the lightweight requirements of complex engineering structures, this study employs the H_∞ optimal control theory to pursue the absolute minimization and suppression of the global maximum amplitude of the primary structure under stringent total mass constraints.

3.1 Min-Max Objective Function and Physical Boundary Constraints

The H_∞ norm optimization for structural vibration control is essentially the minimization of the worst-case resonance response that the system may encounter across the entire frequency spectrum. According to the classical fixed-point theory, the optimal boundary for global vibration suppression is achieved when the two adjacent resonant peaks of the steady-state amplitude-frequency response curve reach an iso-amplitude state. To this end, this study constructs an objective function F_{obj} centered on the Min-Max criterion, aiming to identify the optimal dynamic parameter matrix $\boldsymbol{X} = [m_s, m_t, k_a]$ that minimizes the global maximum displacement response of the primary structure. The objective function is formulated as $F_{obj}(\boldsymbol{X}) = \min(\max_\omega |X_1(\omega, \boldsymbol{X})|)$, where $X_1(\omega, \boldsymbol{X})$ represents the steady-state displacement transfer function of the primary structure.

During the parameter optimization process, the system is subjected to dual constraints derived from physical manufacturability and lightweighting objectives. First, the total physical mass of the metastructure is restricted to $25kg$, satisfying the condition $2m_s + m_t \leq 25kg$. Second, as the top mass m_t serves as the load-bearing base for the tuning spring and the articulation pivot for the linkages, its physical manufacturing lower bound is set to $m_t \geq 0.5kg$ to ensure the structural integrity and stiffness of the overall assembly under high-frequency excitation. Furthermore, the tuning spring stiffness k_a is constrained within $[K_{min}, K_{max}]$ to comprehensively cover the required tuning workspace around the target resonance frequency. The resulting H_∞ optimized frequency response and the evolutionary trajectories of the functional and dead masses are presented in Figure 2, reflecting the convergence of the equivalent apparent mass.

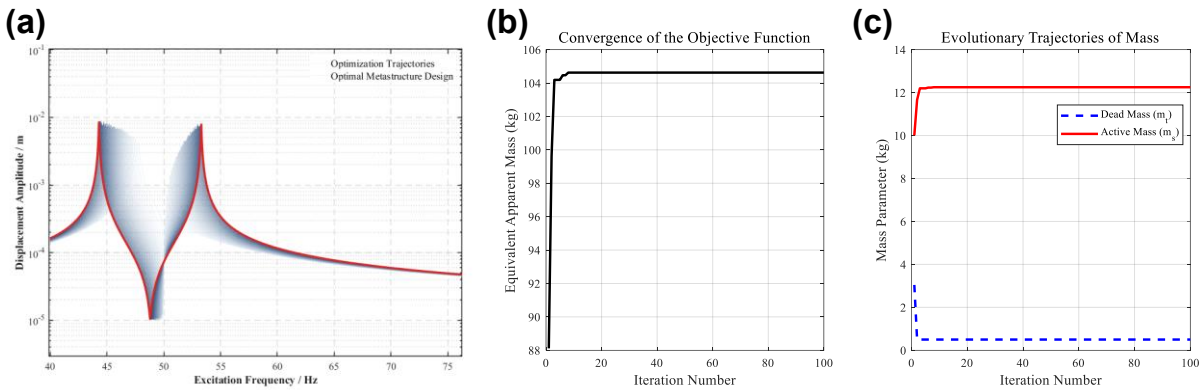


Figure 2: Optimization and Evolution. (a) Optimized frequency response function (FRF). (b) Convergence of equivalent apparent mass during the optimization process. (c) Evolutionary trajectories of the active and static masses.

3.2 Implementation of Parameter Optimization via Particle Swarm Algorithm

Due to the presence of cross-coupling terms in the dynamic matrices of the ungrounded inerter system, the objective function exhibits highly non-convex characteristics within the three-dimensional parameter space. Consequently, traditional gradient-based analytical methods are prone to stagnate in local minima. To overcome this, this section introduces the Particle Swarm Optimization (PSO) algorithm to implement a global search for the optimal parameters.

During the execution of the algorithm, each virtual particle represents a potential configuration of the metastructure's mass and stiffness. Driven by the Lagrangian dynamic model, the particle swarm evaluates the fitness value—defined as the global peak resonance amplitude of the system. Each particle updates its search velocity and spatial coordinates based on its individual historical best position P_{best} and the global historical best position G_{best}. The update laws for velocity and position are formulated as:

$$v_i^{t+1} = wv_i^t + c_1 r_1 (P_{best} - x_i^t) + c_2 r_2 (G_{best} - x_i^t) \tag{8}$$
$$x_i^{t+1} = x_i^t + v_i^{t+1}$$

The computation terminates when the algorithm reaches the maximum number of iterations or when the convergence error of the global optimum falls below a predefined tolerance, at which point the global optimal physical parameter matrix is output.

3.3 Optimization Results and Mass Evolution Analysis

By integrating the theoretical model into the PSO algorithm for iterative computation, clear parameter evolutionary trajectories and global optimal solutions are obtained. A monotonic convergence trend is observed throughout the evolution process: as iterations progress, the algorithm asymptotically pushes the flanking mass m_s toward the upper bound of the total mass constraint, while simultaneously suppressing the top mass m_t to its lower physical manufacturing limit of $0.5kg$.

This evolutionary outcome aligns perfectly with the underlying kinematic essence of inertial amplification. Within the system's equivalent mass mapping matrix, the axial motion of the top mass m_t lacks any geometric amplification effect. Given a fixed total mass budget, any increase in the proportion of m_t inevitably curtails the mass quota available for kinematic amplification. Consequently, in the optimal trade-off to achieve H_∞ suppression, the PSO algorithm makes a deliberate physical decision to minimize the top mass while maximizing the flanking masses.

Ultimately, the global optimal parameters identified by the algorithm are: tuning stiffness $k_a = N/m$, single-side flanking mass $m_s = 12.25\ kg$, and top mass $m_t = 0.5\ kg$. In this extreme state, facilitated by the specific geometric inclination angles, the minuscule added physical mass activates a substantial apparent inertia of up to $104.6\ kg$. While maintaining structural stability, this optimal parameter matrix transforms the absorber into a targeted energy sink within the designated frequency band, providing the parametric foundation for achieving the ultimate suppression of the primary structure's global resonance.

4 COMPARATIVE PERFORMANCE EVALUATION

Following the completion of the dynamic parameter optimization for the ungrounded inertial metastructure, this chapter aims to validate the accuracy of the analytical model through three-dimensional finite element analysis (FEA). Furthermore, a comprehensive evaluation is conducted to assess the performance of the proposed structure in terms of frequency-domain peak suppression and time-domain energy dissipation under stringent lightweighting constraints.

4.1 Frequency-Domain Validation of the Analytical Model

To verify the accuracy of the analytical model for the ungrounded inerter system, this study first constructed a three-dimensional solid model of an industrial piping primary structure using the ANSYS finite element platform. Modal analysis results indicate that the fundamental flexural resonance frequency of the uncontrolled pipe is precisely anchored at $48.8Hz$, with an extracted equivalent modal mass as high as $4800\ kg$. These substantial baseline physical parameters constitute the stringent boundary conditions for the subsequent vibration suppression design; specifically, the proposed metastructure must operate effectively under a lightweight constraint of only approximately 0.5% $(25\ kg)$ of the primary structure's mass.

Upon characterizing the dynamic features of the primary structure, the global optimal physical parameter matrix—obtained via the Particle Swarm Optimization (PSO) algorithm—was assigned to the 3D solid model of the inertial metastructure. A steady-state harmonic forced vibration was then applied to the coupled system. By extracting the FEA frequency sweep data and comparing it with the theoretical analytical solutions, it can be observed that the two steady-state amplitude-frequency response curves achieve excellent agreement across the entire observation band. This high-fidelity frequency-domain alignment not only validates the absolute rigor of extracting equivalent apparent inertia via the Lagrangian method and constructing the ungrounded impedance matrix, but also demonstrates that the proposed structure can accurately replicate the theoretically predicted dynamic behavior under realistic physical boundaries. The fundamental modal characterization of the uncontrolled pipe and the high-fidelity alignment between analytical predictions and FEA simulations are shown in Figure 3.

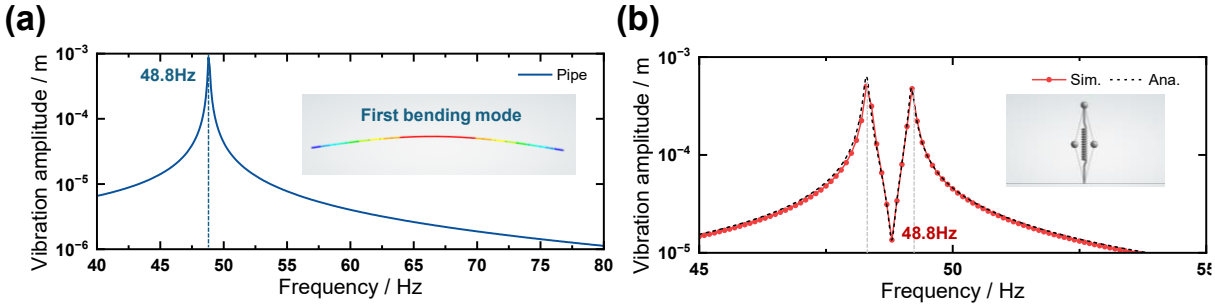


Figure 3: System Characterization and Model Validation. (a) Fundamental flexural mode shape and FRF of the uncontrolled pipe. (b) Comparison between analytical predictions and FEA simulation results.

4.2 Performance of Ultimate Suppression for Global Peak Respons

The core evaluation metric for frequency-domain response lies in the absolute reduction of the global maximum resonance amplitude. For the uncontrolled piping system, the peak displacement extracted at the target resonance frequency of $48.8Hz$ reaches an absolute magnitude of $9.41 \times 10^{-4}m$. Such a high-risk stress response is highly susceptible to inducing structural fatigue during engineering service. Upon integrating the inertial metastructure—with a total mass of only $25\ kg$—the global maximum steady-state response of the system across the entire frequency band is forcibly suppressed to $5.03 \times 10^{-4}m$, representing a drastic absolute reduction of up to 46.5% (see Figure 4(a)).

Under ungrounded boundary conditions, constrained by the minuscule top mass m_t, the system does not exhibit a significant shift in its dynamic poles. However, the substantial apparent inertia of up to $104.6\ kg$ acts as a highly efficient localized energy sink within an extremely narrow engineering bandwidth. This dynamic mechanism—which circumvents the traditional reliance on large masses for bandgap broadening and instead implements a local Min-Max amplitude flattening—perfectly fulfills the engineering objectives of H_∞ norm optimization. This data intuitively demonstrates that the proposed rhombus metastructure can achieve the ultimate suppression of the primary structure's global extreme displacements at a minimal physical cost.

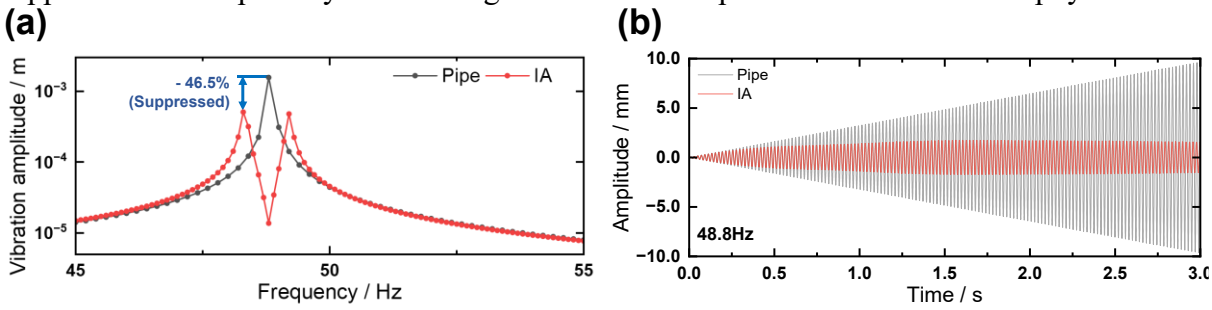


Figure 4: Performance Assessment. (a) Comparison of FRFs with and without the metastructure (46.5% peak reduction). (b) Transient displacement responses under 48.8 Hz harmonic excitation.

4.3 Transient Time-Domain Response and Energy Dissipation Characteristics

To comprehensively evaluate the energy absorption performance and dynamic robustness of the inertial metastructure under complex transient impacts, this section further conducts a time-domain transient dynamic analysis. First, a harmonic excitation load is applied to the system at the target resonance frequency of $48.8Hz$. The results indicate that the displacement response of the uncontrolled primary structure diverges rapidly and maintains a long-term presence within a high-risk amplitude range. In contrast, for the piping system equipped with the inertial metastructure, following a minimal initial startup period, the substantial equivalent apparent inertia intervenes rapidly and powerfully extracts kinetic energy from the primary structure. This forces the global vibration envelope to decay rapidly and converge within an extremely low steady-state safety displacement threshold (see Figure 4(b)).

To further verify the operational stability of the system at critical nodal points across the frequency spectrum, this study extracted the transient time-domain response curves at three characteristic frequencies: the left-hand derivative resonant peak, the anti-resonance valley, and the right-hand derivative resonant peak. At these three extreme frequency points (see Figure 5), which are most susceptible to inducing dynamic instability, the metastructure consistently exhibits exceptionally stable and rapid energy dissipation characteristics. Regardless of the excitation frequency shifting within the effective control bandwidth, the system shows no signs of high-frequency beating oscillations or divergent loss of control. These time-domain matrix data

thoroughly validate that the ungrounded inertial metastructure, while achieving Min-Max suppression in the frequency domain, simultaneously possesses superior transient energy dissipation capabilities.

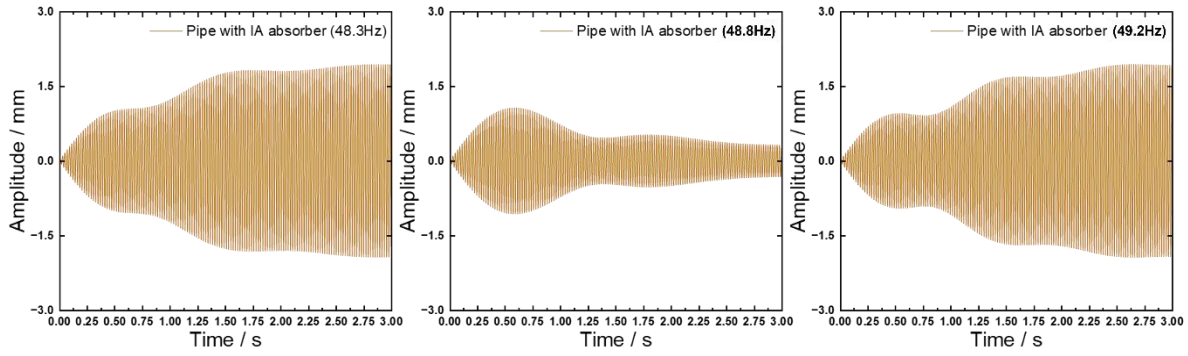


Figure 5: Transient Stability at Characteristic Frequencies.

5 CONCLUSION

Addressing the challenge of low-frequency vibration control in complex engineering piping systems under stringent lightweighting constraints, this study proposes and validates an ungrounded rhombus inertial metastructure absorber. Through rigorous kinematic derivation, heuristic algorithm optimization, and three-dimensional finite element simulations, we have systematically demonstrated the feasibility and superior performance of this structure in achieving ultimate suppression of the primary structure's global resonance amplitude with minimal added mass.

First, this study established a dynamic analytical model of the metastructure based on the Lagrange energy method, which unveiled the underlying physical mechanisms of the ungrounded inerter system. Under the strict constraint of a total added mass not exceeding $25\ kg$, the Particle Swarm Optimization (PSO) algorithm was employed to implement an H_∞ optimal control strategy. The parameter evolutionary results demonstrate that by minimizing the top mass—which lacks geometric amplification—and maximizing the flanking masses, the algorithm successfully leverages specific geometric inclination angles to activate a substantial equivalent apparent inertia of up to $104.6\ kg$. This parametric configuration maintains a narrow engineering bandwidth while constructing a highly efficient localized core for energy dissipation. Second, the three-dimensional finite element simulation results achieve high-fidelity alignment with the theoretical analytical solutions across the entire frequency spectrum, verifying the absolute accuracy of the dynamic modeling. For the primary piping structure with a fundamental flexural resonance frequency near $48.8Hz$, the designed inertial metastructure—with a minimal mass ratio of only approximately 0.5%—achieved a radical absolute reduction of 46.5% in the system's global maximum steady-state response, without inducing significant shifts in the macroscopic poles. Furthermore, the transient time-domain dynamic analysis confirms that the structure exhibits rapid vibration energy extraction and robust dynamic stability at both the target resonance and critical characteristic frequencies, perfectly fulfilling the engineering objective of vibration suppression under extreme lightweighting conditions.

Finally, although this study achieves exceptional Min-Max suppression of peak amplitudes under stringent mass boundaries, the purely linear ungrounded mechanism imposes an intrinsic constitutive limitation on the absolute bandwidth of the system's bandgap. Future research will focus on integrating nonlinear restoring force elements into the inertial amplification network. By exploring nonlinear bifurcation and resonance peak shifting effects, we aim to overcome the inter-peak repulsion bottleneck inherent in linear dynamic matrices. The objective is to

maintain extreme structural lightweighting while achieving broadband low-frequency vibration attenuation for complex wideband excitation environments, thereby providing a higher-order theoretical paradigm for the structural dynamic design of next-generation aerospace and rail transit equipment.

REFERENCES

[1] Elias S, Beer M. Vibration control and energy harvesting of offshore wind turbines installed with TMDI under dynamical loading[J]. Engineering Structures, 2024, 315: 118459.

[2] Colherinhas G B, de Morais M V G, Petrini F. Global vibration control of offshore wind turbines with a flexible monopile foundation using a pendulum-tuned mass damper: Risk mitigation and performance incrementation[J]. Ocean Engineering, 2024, 297: 117168.

[3] Marrazzo P R, Montuori R, Nastri E, et al. Advanced seismic retrofitting with high-mass-ratio Tuned Mass Dampers[J]. Soil Dynamics and Earthquake Engineering, 2024, 179: 108544.

[4] Sarkar S, Fitzgerald B. Design of tuned mass damper fluid inerter for wind-induced vibration control of a tall building[J]. Journal of Structural Engineering, 2024, 150(3): 04023242.

[5] Jin Y, Torrent D, Rouhani B D, et al. The 2024 phononic crystals roadmap[J]. Journal of Physics D: Applied Physics, 2025, 58(11): 113001.

[6] Lee J, Kim Y Y. Elastic metamaterials for guided waves: from fundamentals to applications[J]. Smart Materials and Structures, 2023, 32(12): 123001.

[7] Contreras N, Zhang X, Hao H, et al. Application of elastic metamaterials/meta-structures in civil engineering: a review[J]. Composite Structures, 2024, 327: 117663.

[8] Xu L, Yang Z, Zhang Z, et al. Lightweight composite meta-lattice structures with inertial amplification design for broadband low-frequency vibration mitigation[J]. Composites Part B: Engineering, 2025, 292: 112091.

[9] Xu L, Wu R, Zhang Z, et al. Hierarchical meta-lattice structures with inertial amplification design for broadband low-frequency vibration mitigation[J]. Engineering Structures, 2026, 346: 121601.

[10] Wall I P, Amoozgar M R, Popov A A. Aeroelasticity of an aircraft wing with nonlinear energy sink[J]. Aerospace Science and Technology, 2024, 155: 109684.

[11] Saeed A S, Abdul Nasar R, Al-Shudeifat M A. A review on nonlinear energy sinks: designs, analysis and applications of impact and rotary types[J]. Nonlinear Dynamics, 2023, 111(1): 1-37.

[12] Zhou J, Dou L, Wang K, et al. A nonlinear resonator with inertial amplification for very low-frequency flexural wave attenuations in beams[J]. Nonlinear Dynamics, 2019, 96(1): 647-665.

[13] Ma H, Cheng Z, Shi Z, et al. Structural vibration mitigation via an inertial amplification mechanism based absorber[J]. Engineering Structures, 2023, 295: 116764.